



UNIVERSITÀ DI SIENA 1240

dedica a ...

Abstract

Lorem ipsum dolor sit amet, consectetur adipiscing elit. Ut purus elit, vestibulum ut, placerat ac, adipiscing vitae, felis. Curabitur dictum gravida mauris. Nam arcu libero, nonummy eget, consectetur id, vulputate a, magna. Donec vehicula augue eu neque. Pellentesque habitant morbi tristique senectus et netus et malesuada fames ac turpis egestas. Mauris ut leo. Cras viverra metus rhoncus sem. Nulla et lectus vestibulum urna fringilla ultrices. Phasellus eu tellus sit amet tortor gravida placerat. Integer sapien est, iaculis in, pretium quis, viverra ac, nunc. Praesent eget sem vel leo ultrices bibendum. Aenean faucibus. Morbi dolor nulla, malesuada eu, pulvinar at, mollis ac, nulla. Curabitur auctor semper nulla. Donec varius orci eget risus. Duis nibh mi, congue eu, accumsan eleifend, sagittis quis, diam. Duis eget orci sit amet orci dignissim rutrum.

Nam dui ligula, fringilla a, euismod sodales, sollicitudin vel, wisi. Morbi auctor lorem non justo. Nam lacus libero, pretium at, lobortis vitae, ultricies et, tellus. Donec aliquet, tortor sed accumsan bibendum, erat ligula aliquet magna, vitae ornare odio metus a mi. Morbi ac orci et nisl hendrerit mollis. Suspendisse ut massa. Cras nec ante. Pellentesque a nulla. Cum sociis natoque penatibus et magnis dis parturient montes, nascetur ridiculus mus. Aliquam tincidunt urna. Nulla ullamcorper vestibulum turpis. Pellentesque cursus luctus mauris.

Ringraziamenti

Lorem ipsum dolor sit amet, consectetur adipiscing elit. Ut purus elit, vestibulum ut, placerat ac, adipiscing vitae, felis. Curabitur dictum gravida mauris. Nam arcu libero, nonummy eget, consectetur id, vulputate a, magna. Donec vehicula augue eu neque. Pellentesque habitant morbi tristique senectus et netus et malesuada fames ac turpis egestas. Mauris ut leo. Cras viverra metus rhoncus sem. Nulla et lectus vestibulum urna fringilla ultrices. Phasellus eu tellus sit amet tortor gravida placerat. Integer sapien est, iaculis in, pretium quis, viverra ac, nunc. Praesent eget sem vel leo ultrices bibendum. Aenean faucibus. Morbi dolor nulla, malesuada eu, pulvinar at, mollis ac, nulla. Curabitur auctor semper nulla. Donec varius orci eget risus. Duis nibh mi, congue eu, accumsan eleifend, sagittis quis, diam. Duis eget orci sit amet orci dignissim rutrum.

Nam dui ligula, fringilla a, euismod sodales, sollicitudin vel, wisi. Morbi auctor lorem non justo. Nam lacus libero, pretium at, lobortis vitae, ultricies et, tellus. Donec aliquet, tortor sed accumsan bibendum, erat ligula aliquet magna, vitae ornare odio metus a mi. Morbi ac orci et nisl hendrerit mollis. Suspendisse ut massa. Cras nec ante. Pellentesque a nulla. Cum sociis natoque penatibus et magnis dis parturient montes, nascetur ridiculus mus. Aliquam tincidunt urna. Nulla ullamcorper vestibulum turpis. Pellentesque cursus luctus mauris.

Contents

Introduction	xi
1 The Standard Model, Higgs Boson and New Scalar Particles	1
1.1 The Standard Model	1
1.2 The Higgs Boson	1
1.3 New Scalar Particles	1
1.3.1 Study of the interference effects	1
2 The CMS experiment at LHC	3
2.1 The Large Hadron Collider	3
2.2 The Compact Muon Solenoid experiment	3
3 Monte Carlo event simulation	5
4 Event Reconstruction	7
5 High mass resonances searching	9
5.1 Introduction	9
5.2 Discriminating variable	10
5.3 Signal interpretation	10
5.4 Opposite Flavor final state	15
5.5 Same Flavor final state	28
5.5.1 Drell-Yan control region	30
5.5.2 Top control region	35
6 Results and Interpretation	39
A Special commands	41

Introduction

Lorem ipsum dolor sit amet, consectetur adipiscing elit. Ut purus elit, vestibulum ut, placerat ac, adipiscing vitae, felis. Curabitur dictum gravida mauris. Nam arcu libero, nonummy eget, consectetur id, vulputate a, magna. Donec vehicula augue eu neque. Pellentesque habitant morbi tristique senectus et netus et malesuada fames ac turpis egestas. Mauris ut leo. Cras viverra metus rhoncus sem. Nulla et lectus vestibulum urna fringilla ultrices. Phasellus eu tellus sit amet tortor gravida placerat. Integer sapien est, iaculis in, pretium quis, viverra ac, nunc. Praesent eget sem vel leo ultrices bibendum. Aenean faucibus. Morbi dolor nulla, malesuada eu, pulvinar at, mollis ac, nulla. Curabitur auctor semper nulla. Donec varius orci eget risus. Duis nibh mi, congue eu, accumsan eleifend, sagittis quis, diam. Duis eget orci sit amet orci dignissim rutrum.

Nam dui ligula, fringilla a, euismod sodales, sollicitudin vel, wisi. Morbi auctor lorem non justo. Nam lacus libero, pretium at, lobortis vitae, ultricies et, tellus. Donec aliquet, tortor sed accumsan bibendum, erat ligula aliquet magna, vitae ornare odio metus a mi. Morbi ac orci et nisl hendrerit mollis. Suspendisse ut massa. Cras nec ante. Pellentesque a nulla. Cum sociis natoque penatibus et magnis dis parturient montes, nascetur ridiculus mus. Aliquam tincidunt urna. Nulla ullamcorper vestibulum turpis. Pellentesque cursus luctus mauris.

Chapter 1

The Standard Model, Higgs Boson and New Scalar Particles

1.1 The Standard Model

1.2 The Higgs Boson

1.3 New Scalar Particles

1.3.1 Study of the interference effects

Chapter 2

The CMS experiment at LHC

2.1 The Large Hadron Collider

2.2 The Compact Muon Solenoid experiment

Chapter 3

Monte Carlo event simulation

Chapter 4

Event Reconstruction

Chapter 5

High mass resonances searching

5.1 Introduction

The search for a new resonance X is described in this chapter.

The main production mode for the Higgs boson particle over the all mass spectrum is the gluon-gluon fusion (ggH) process. At a center-of-mass energy of 13 TeV the ggH cross section for a Higgs boson mass (m_H) of 125 GeV is 43.92 pb [3], that is almost one order of magnitude larger than the second process in terms of cross section at that mass, VBF, with 3.748 pb [3]. The gluon-gluon fusion cross section decreases with m_H but the VBF/ggH cross section ratio increases with the mass, making the VBF production mechanism more and more important as m_H approaches to high values.

The signal samples are interpreted in terms of the EWK singlet model described in Sec 5.3 below. The Higgs boson width and lineshape is reweighted at generator level according to the parameters defined in the model. The interference effects between the ggH signal, the ggWW background and SM Higgs boson, that are expected to slightly change the lineshape of the signal distribution, have been fully taken into account, as detailed in Sec. 5.3. A similar treatment is also applied for the interference between the VBF high mass signal, the VBF SM Higgs and the quark initiated WW+2 quarks background. The interference between the $W^+W^- \rightarrow 2\ell 2\nu$ and $ZZ \rightarrow 2\ell 2\nu$ is negligible due to the different phase space characteristic of these processes.

The analysis strategy for the high mass search with 2016 data in the $W^+W^- \rightarrow 2\ell 2\nu$ decay channel is similar to the previous high mass analysis with 2015 data [1], but has several improvements.

The analysis is divided in two parts:

- the opposite-flavour final state, $e^\pm \mu^\mp$,
- the same-flavour final state, e^+e^- and $\mu^+\mu^-$.

In the opposite-flavour final state four different jets-categories are defined: the 0-jet, the 1-jet, the 2-jet non VBF and finally the VBF. The 2-jet non-VBF category is new with respect to previous analysis with 2015 data.

In the same-flavour final state only the VBF category is considered. Indeed, the

only the VBF selection cuts are sufficiently tight to reduce the overwhelming Z+jets background to a manageable level.

5.2 Discriminating variable

This analysis is a shape analysis, meaning that after applying selection cuts we do not simply count events, but rather we fit a data histogram of a discriminating variable with the sum of signal and background templates, and extract the signal yield from the fit. The variable with the best discriminating value would be the invariant mass of the four lepton, which is not possible to reconstruct in the WW channel due to neutrinos.

For the Higgs boson in WW analysis, the shape analysis is based on two-dimensional templates of $m_{\ell\ell}$ versus m_T^H , where the transverse mass m_T^H variable is defined as

$$m_T^H = \sqrt{2p_T^{\ell\ell} E_T^{\text{miss}} (1 - \cos\Delta\phi(\ell\ell, \vec{p}_T^{\text{miss}}))} \quad (5.1)$$

where $\Delta\phi(\ell\ell, \vec{p}_T^{\text{miss}})$ is the azimuthal angle between the dilepton momentum and \vec{p}_T^{miss} .

However m_T^H (and also $m_{\ell\ell}$) is not very sensitive to the signal mass hypothesis, so a new variable m_T^I defined as the visible mass,

$$m_T^I = \sqrt{(p_{\ell\ell} + E_T^{\text{miss}})^2 - (\vec{p}_{\ell\ell} + \vec{p}_T^{\text{miss}})^2} \quad (5.2)$$

has been introduced to discriminate better the high mass X signals generate at different masses. The distribution of the variables defined above are shown in Fig. 5.1, where it is visible the better power of m_T^I in discriminating different mass hypotheses respect the other variable.

5.3 Signal interpretation

The signal is interpreted in terms of the electroweak singlet model, representing a scalar mixing with the 125 GeV Higgs boson. This model relies on two parameters: the scale factor of the couplings of the high mass resonance with respect to the SM, C' , and the branching fraction of the electroweak singlet to non-SM decays modes, BR_{new} . The electroweak singlet signal strength, μ' and the modified width, Γ' , are related with the parameters in the model by the following equations:

$$\mu' = C'^2 \cdot (1 - BR_{\text{new}}) \quad (5.3)$$

$$\Gamma' = \Gamma_{\text{SM}} \cdot \frac{C'^2}{1 - BR_{\text{new}}} \quad (5.4)$$

The available Higgs signal samples for different mass hypothesis have been reweighted according to this model. At the moment only the $BR_{\text{new}} = 0$ hypothesis has been investigated while we tested different C' values. In Fig. 5.2 are shown the $m_{\ell\ell}$ and m_T templates corresponding to a Higgs boson mass of 700 GeV for three different C' values: $C' = 1$, corresponding to the SM Higgs decay width, $C' = 0.5$, corresponding to $\Gamma' = 2.5 \cdot 10^{-2} \Gamma_{\text{SM}}$, and $C' = 0.1$, corresponding to $\Gamma' = 10^{-2} \Gamma_{\text{SM}}$. A value of $BR_{\text{new}} = 0$ is considered in all cases. We note that the signal shape is not very sensitive to different C' values.

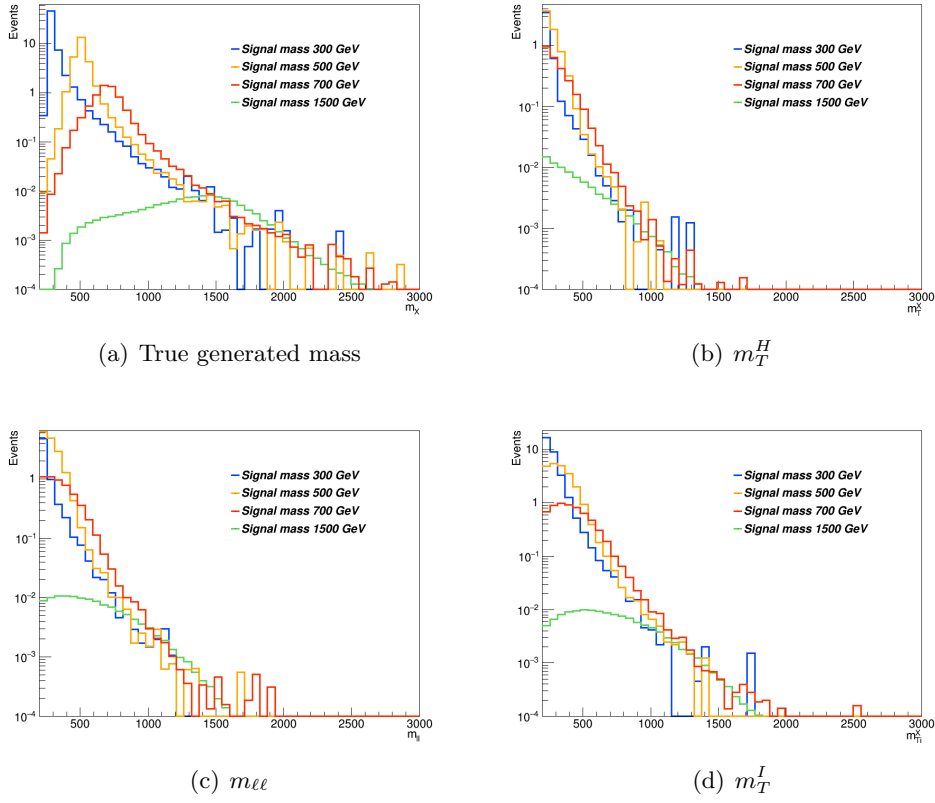


Figure 5.1. Distributions of the generated mass, m_T^H , $m_{\ell\ell}$ and m_T^I variables for different X mass hypothesis.

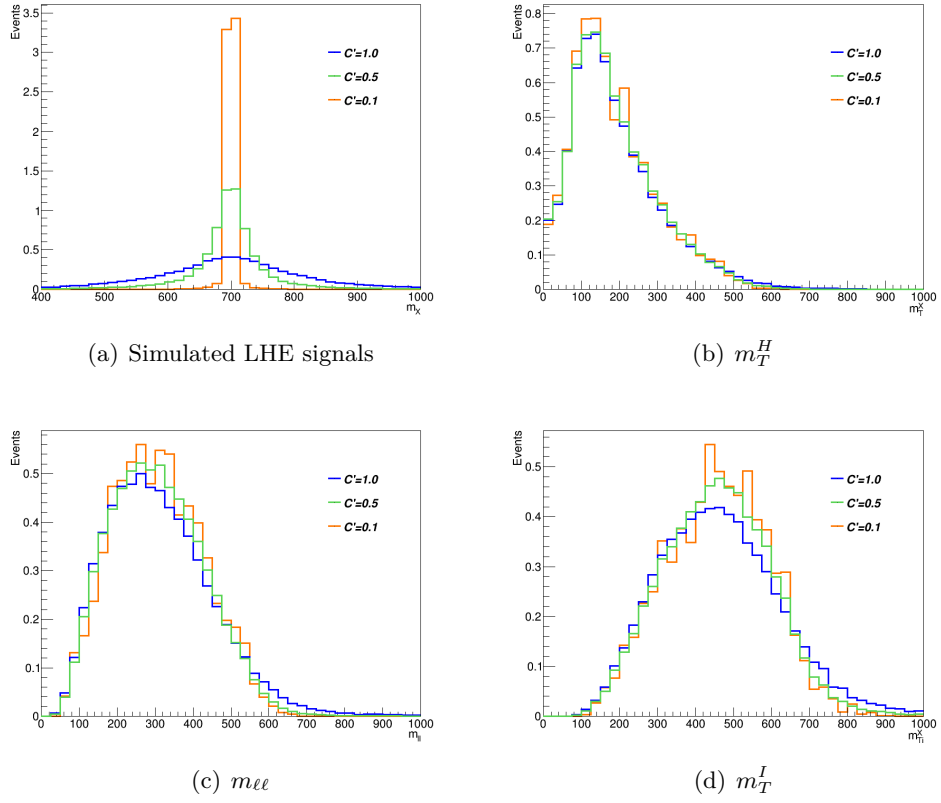


Figure 5.2. Distributions of the signals, the m_T^H , the $m_{\ell\ell}$ and the m_T^I variables at generator level for different values of C' , without any selection.

Study of the Interference effects

When a resonance X , with a non negligible width is considered, it is important to take into account also the interference effects both with the WW background, with same initial and final state, and with the Higgs boson off-shell tail.

In this analysis we take into account the interference effects between the new signal X produced in gluon-gluon fusion and in vector-boson-fusion. The effect of the various interference terms are shown in 5.3 and 5.4 for the two different production mechanism, gluon-gluon fusion and vector-boson.fusion. The contribution of the interference of X with WW background and with Higgs boson have opposite sign and partially cancel out. This cancellation effect is different for different resonance masses. The interference contribution is thus non negligible and is included in the fit.

To prevent possible negative probability distribution function of the interference, during the fit the signal yield is computed as,

$$Yield = \sqrt{\mu} \times (S + B + I) + (\mu - \sqrt{\mu}) \times (S) + (1 - \sqrt{\mu}) \times (B) \quad (5.5)$$

where S is the signal, B the background and I the interference.

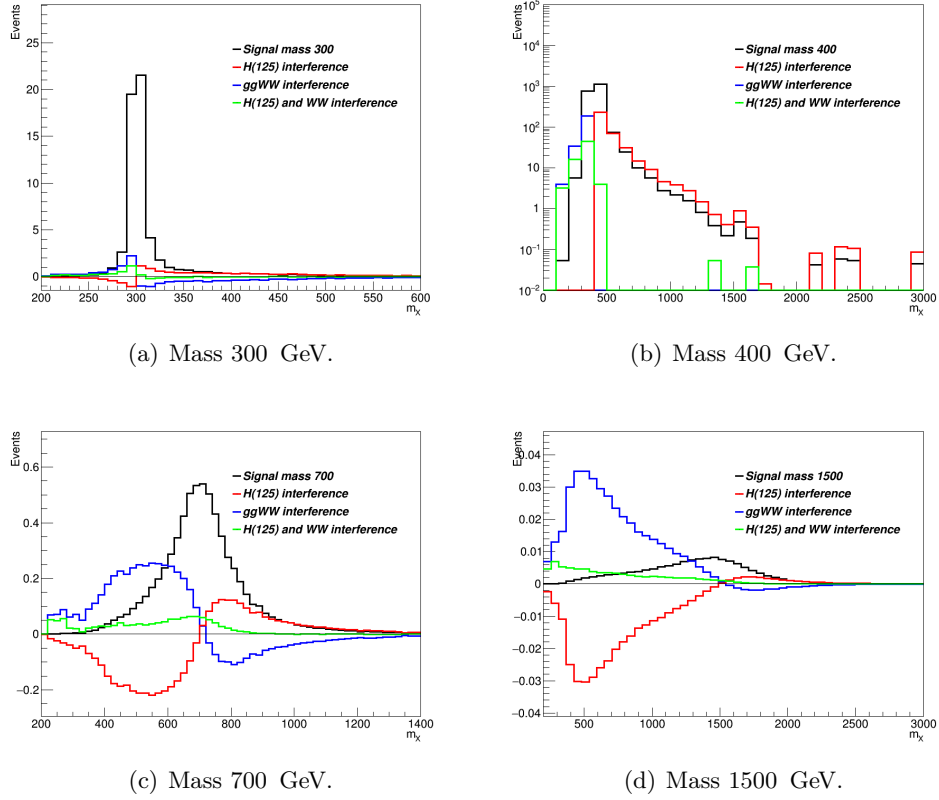


Figure 5.3. Distribution of for the X mass resonance, produced via gluon-gluon fusion for different masses. In black the high mass signal. In red the interference between the high mass signal and the Higgs boson. In blue the interference between the high mass signal and the background. In green the total interference i.e. high mass signal, Higgs boson and background.

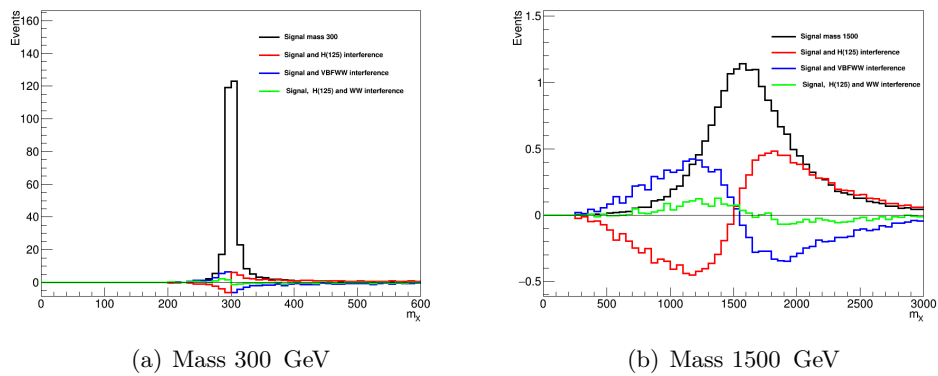


Figure 5.4. Distribution of for the X mass resonance, produced via vector-boson-fusion for different masses. In black the high mass signal. In red the interference between the high mass signal and the Higgs boson. In blue the interference between the high mass signal and the background. In green the total interference i.e. high mass signal, Higgs boson and background.

5.4 Opposite Flavor final state

In this section the analysis for the opposite-flavour final state $W^+W^- \rightarrow \mu^\pm e^\mp 2\nu$ is described.

Signal region

The events are requested to pass single or double lepton triggers, and exactly one electron and one muon are requested to be reconstructed in the event. One of the two leptons is requested to have a p_T greater than 25 GeV, the other is requested to have p_T greater than 20 GeV and both leptons are requested to be well identified and isolated, to reject non-prompt leptons and leptons coming from QCD sources. To suppress background processes with three or more leptons in the final state, such as ZZ , WZ , $Z\gamma$, $W\gamma$ or triboson production, no additional identified and isolated lepton with $p_T > 10$ GeV should be reconstructed. The low dilepton invariant mass region dominated by QCD production of leptons is not considered in the analysis and $m_{\ell\ell}$ is requested to be higher than 50 GeV to reduce the SM Higgs boson ($m_H=125$ GeV) contamination. A moderate MET cut is applied $MET > 20$ GeV due to the presence of neutrinos in the final state searched for. Since a High mass signal is searched for, an $m_T^I > 100$ GeV is applied. A cut on the transverse momentum ($p_T^{\ell\ell} > 30$ GeV) and on the $m_T^H > 60$ GeV are applied against $DY \rightarrow \tau\tau$ background. Finally, against the top background, all jets above 20 GeV are requested not to be identified as b-jets according to the cMVA2 tagger, loose WP. This is the full selection, defined as the “WW OF selection” :

- Two isolated leptons with different charge and flavor ($\mu^\pm e^\mp$);
- p_T of the leading lepton > 25 GeV;
- p_T of the trailing lepton > 20 GeV;
- Third lepton veto: veto events if a third lepton with $p_T > 10$ GeV;
- $m_{\ell\ell} > 50$ GeV, to reduce H(125) contamination;
- $MET > 20$ GeV;
- $m_T^I > 100$ GeV;
- $p_T^{\ell\ell} > 30$ GeV;
- $m_T^H > 60$ GeV;
- no b-tagged (cMVA2 loose WP) jets with $p_T > 20$ GeV;

Events passing the “WW OF selection” are categorized according to the jet multiplicity, counting jets above 30 GeV, to enhance the sensitivity, especially against the top background.

- **0 jet**, no jets are required in the event;

- **1 jet**, exactly 1 jet is required in the event;
- **2 jet**, exactly 2 jets are required in the event and in addition the condition $\Delta\eta_{jj} < 3.5$ **or** $m_{jj} < 500$ GeV;
- **VBF**, exactly 2 jets are required in the event and in addition the condition $\Delta\eta_{jj} > 3.5$ **and** $m_{jj} > 500$ GeV;

where the 2 jet and VBF regions are mutually exclusive by construction.

To extract high mass boson signals in these four categories, the strategy is followed: the m_T^I distribution is fitted as the sum of signal and background templates. Different binnings have been chosen for the m_T^I distributions in the different categories. The binning was chosen to have at least 10 top Monte Carlo events in each bin of the template. The chosen bins are:

- **0/1/2 jet**, [100,150,200,250,300,350,400,450,500,550,600,650,700,750,800,900,1000,2000]
- **VBF**, [100,150,200,250,300,350,400,500,700,1000,2000]

where the first number represents the lower edge of the first bin while the other numbers represent the upper edges. The last bin is an overflow bin.

The m_T^I distributions for the signal regions are presented in the four categories in Figs. 5.5.

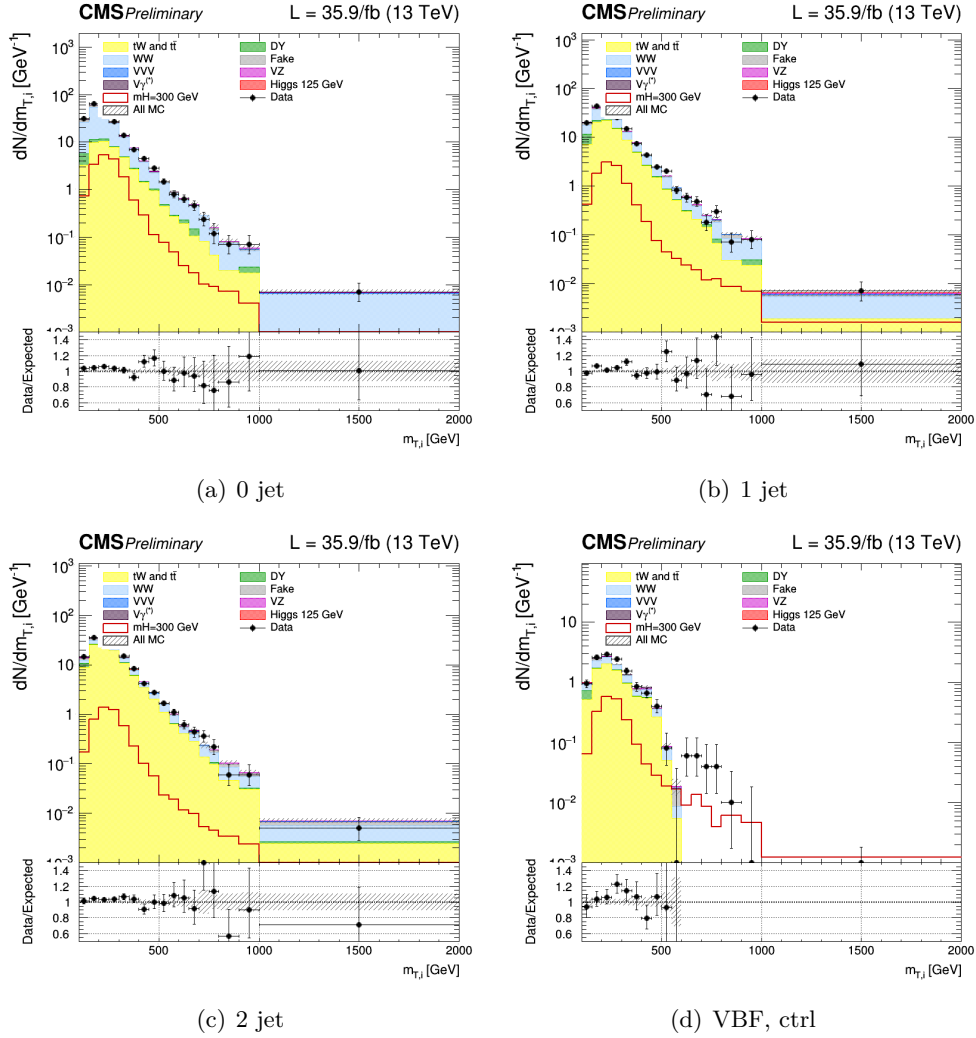


Figure 5.5. Unblinding distributions m_T^I in the signal region for 0, 1, 2 and VBF categories. The signal hypothesis corresponding to m_X of 300 GeV.

Background estimation

The main background processes that affect this signature arise from non-resonant WW production and from top production, including $t\bar{t}$ pairs and single top production (mostly tW), and are estimated using data. Instrumental backgrounds arising from non-prompt leptons in W+jets production and mis-measurement of E_T^{miss} in Drell-Yan events are also estimated from data. The contribution from $W\gamma^*$ is estimated partly from data. The contribution of other sub-dominant backgrounds is obtained directly from simulated samples. The different data-driven background estimations are explained in the following subsections. More precisely top and DY backgrounds normalizations have been extracted directly from data-simulation comparison in specific control regions enriched in either one or the other background separately for the 0, 1, 2 and VBF jet categories, using the rateParam feature of the combine package [ref].

Drell-Yan $\tau\tau$ control region

To normalize the Drell-Yan $\tau\tau$ background to the data, control regions have been defined, as close as possible to the signal region, but enriched in $Z \rightarrow \tau^+\tau^-$. In particular, the “WW OF selection” is used with inverted m_T^H cut, i.e. $m_T^H < 60$. In addition a cut on the invariant mass of the two leptons $50 \text{ GeV} < m_{\ell\ell} < 80 \text{ GeV}$ is requested to exclude possible contribution from non-prompt leptons (low limit) and from $t\bar{t}$ (high limit).

For each signal category, a corresponding Drell-Yan $\tau\tau$ control regions is defined. We thus have 4 total Drell-Yan $\tau\tau$ control regions, for 0 jets, 1 jets, 2 jets and VBF.

The control plots for several variables in a Drell-Yan enriched phase space for the four jets categories are shown in Figs. 5.6, 5.7, 5.8, 5.9. In general there is a good agreement between data and MC.

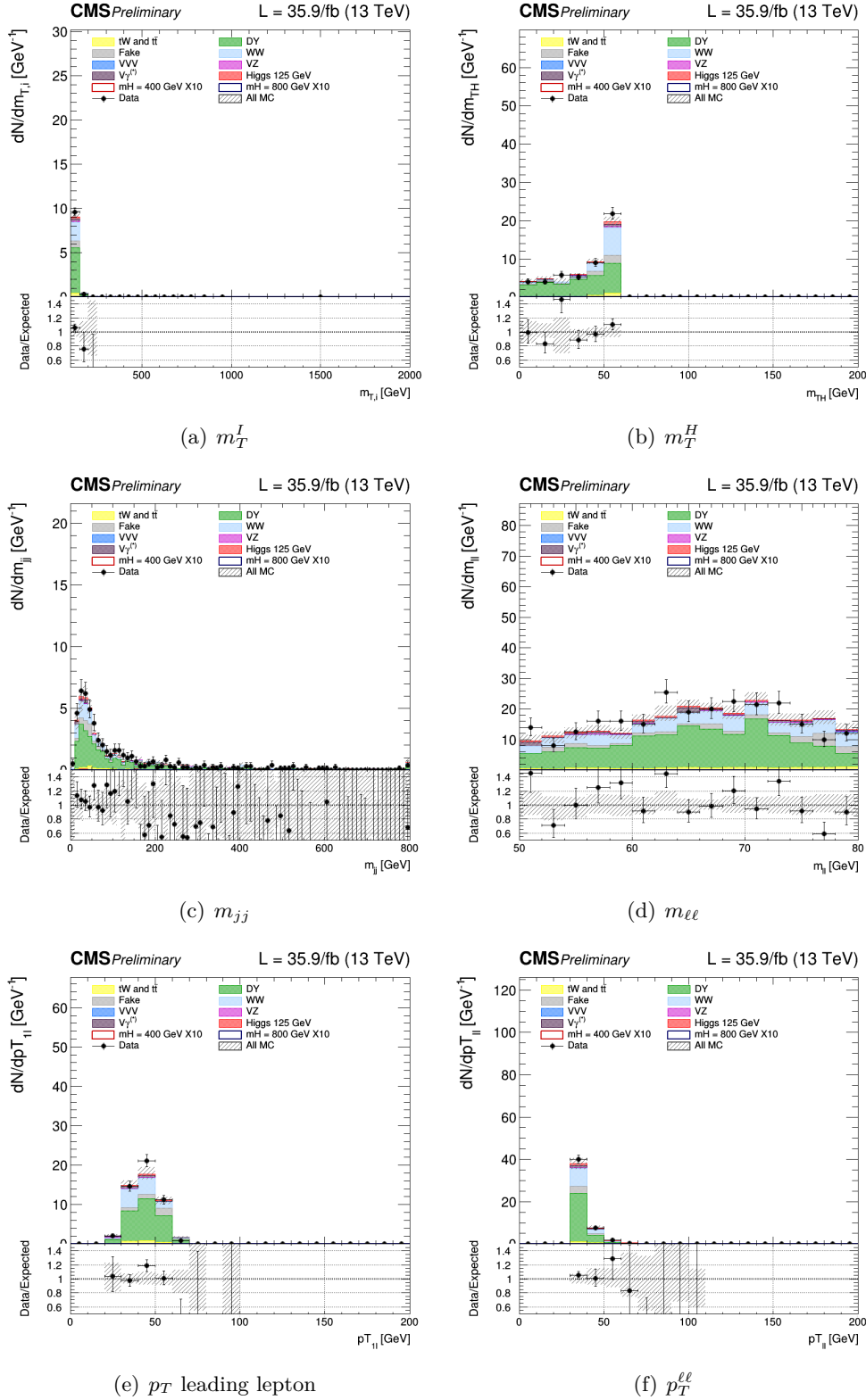


Figure 5.6. Control plots for several variables in a Drell-Yan enriched phase space for events with 0 jet.

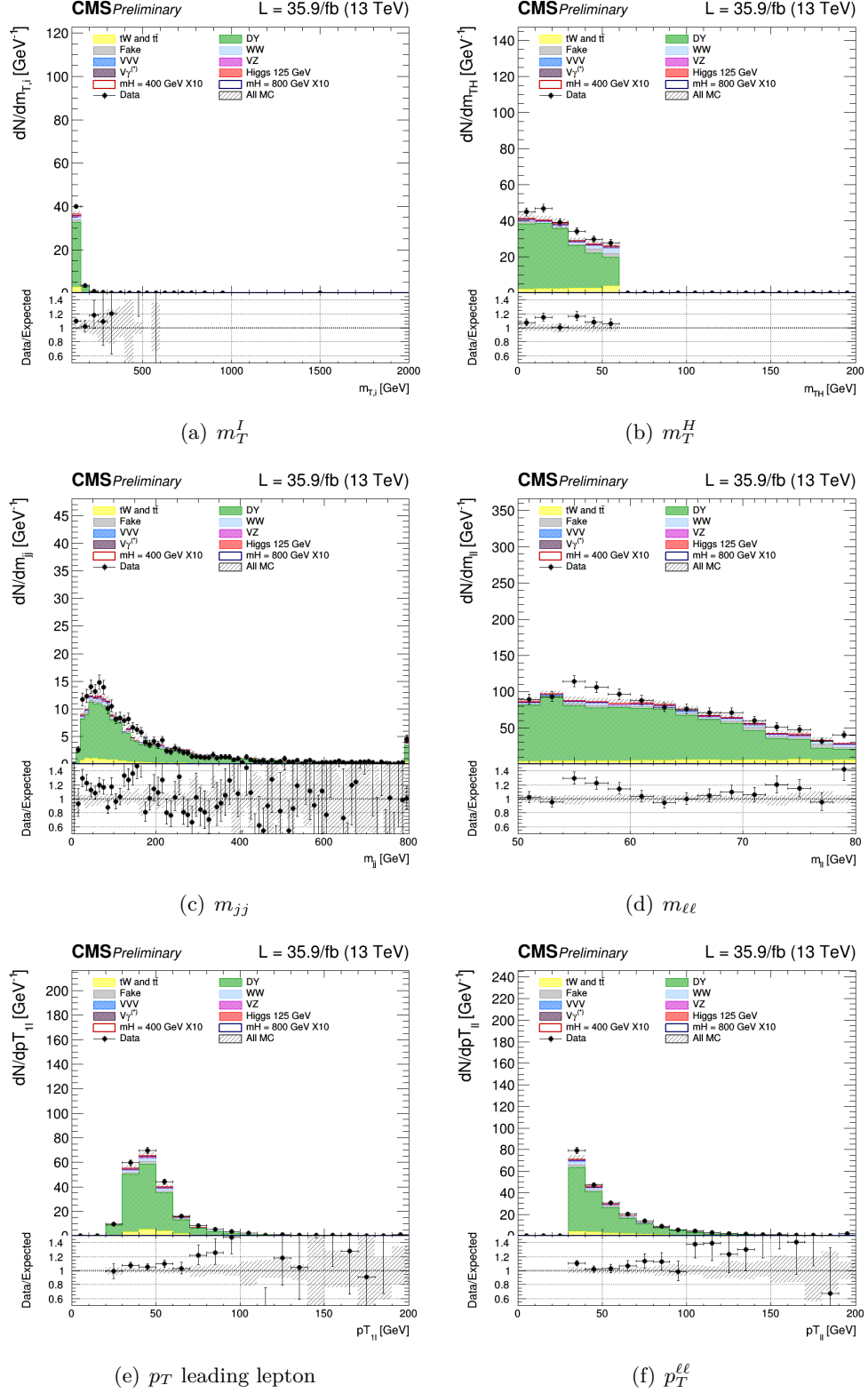


Figure 5.7. Control plots for several variables in a Drell-Yan enriched phase space for events with 1 jet.

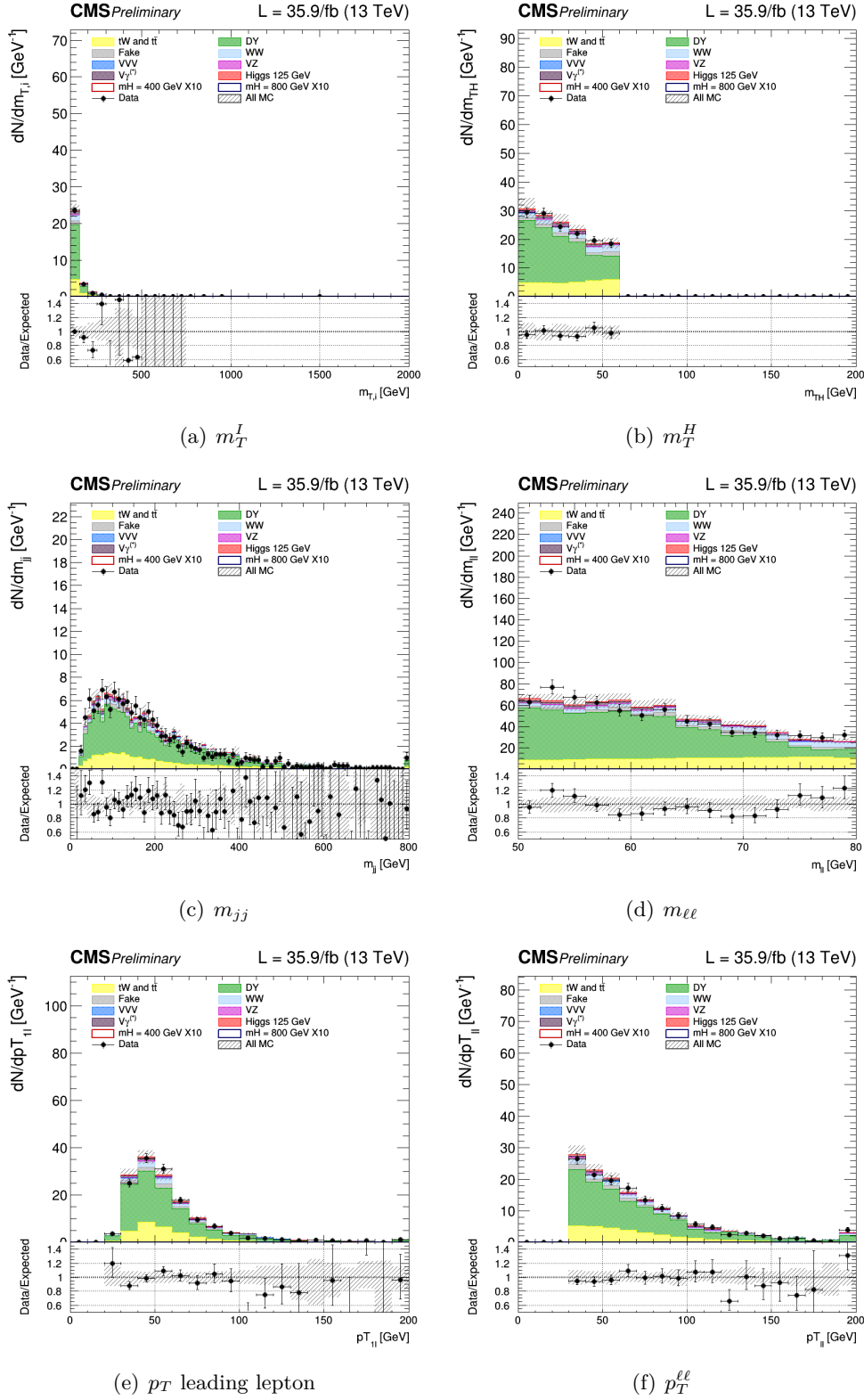


Figure 5.8. Control plots for several variables in a Drell-Yan enriched phase space for events with 2 jet.

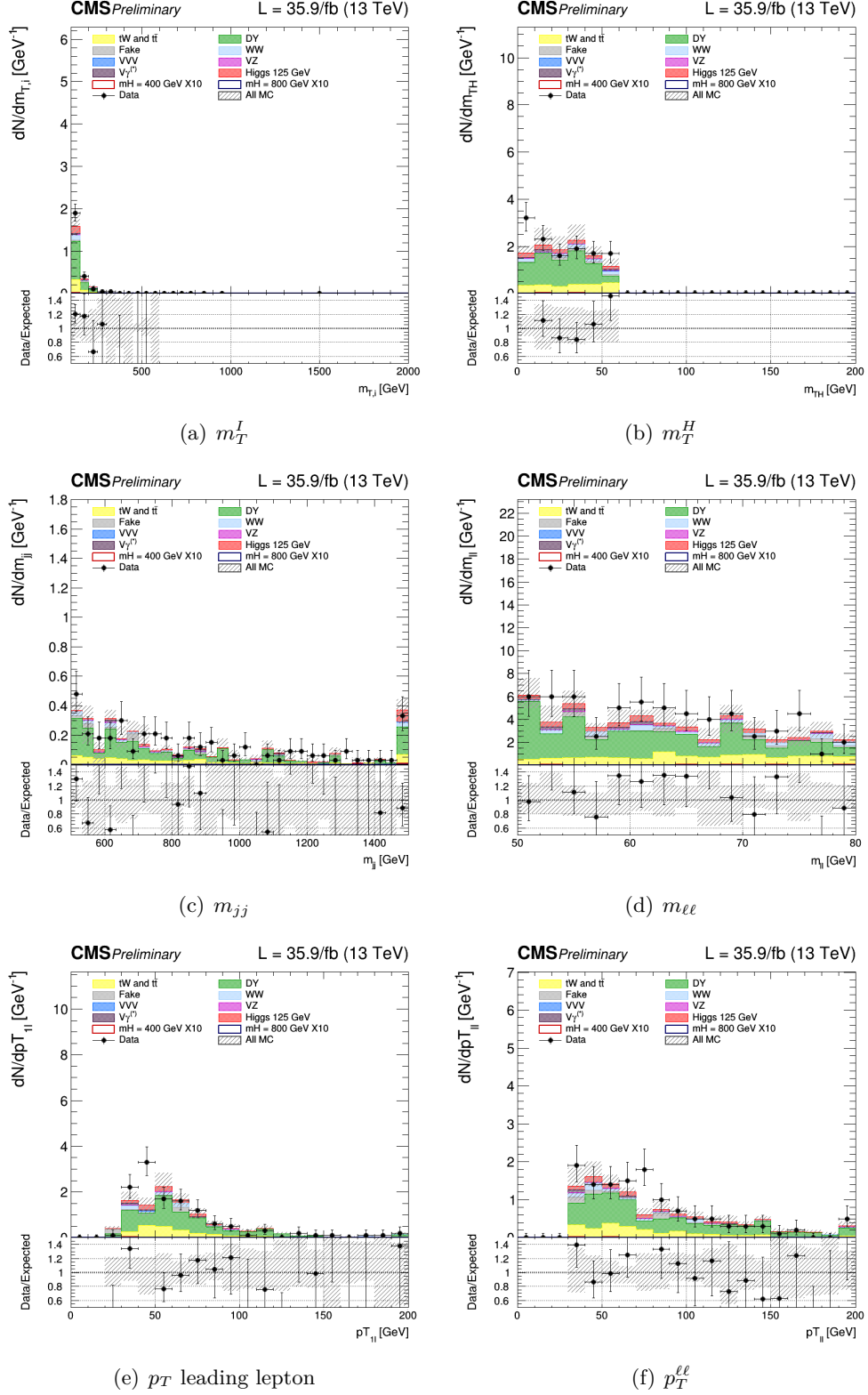


Figure 5.9. Control plots for several variables in a Drell-Yan enriched phase space for events for VBF.

Top control region

Similarly to the Drell-Yan $\tau\tau$ case, control regions are defined for the Top background, and they are used to normalize the top background to data. The “WW OF selection” is used with inversion of the veto on b-jets. In particular the following conditions are imposed to select a top enriched control region for each of the 4 signal regions:

- **0 jet**, at least one b-tagged jet with $20 < p_T < 30$ GeV is required;
- **1 jet**, exactly one b-tagged jet with p_T above 30 GeV is required;
- **2 jet**, exactly 2 jets with at least one of them b-tagged and in addition the condition $\Delta\eta_{jj} < 3.5$ **or** $m_{jj} < 500$ GeV;
- **VBF**, exactly 2 jets with at least one of them b-tagged and in addition the condition $\Delta\eta_{jj} > 3.5$ **and** $m_{jj} > 500$ GeV.

A jet is considered b-tagged if its cMVA_{v2} score is above the threshold defining the loose working point.

The control plots for several variables in a top enriched phase space for events are shown in the Fig. Figs. 5.10, 5.11, 5.12, 5.13. The last bin in the distribution is the overflow.

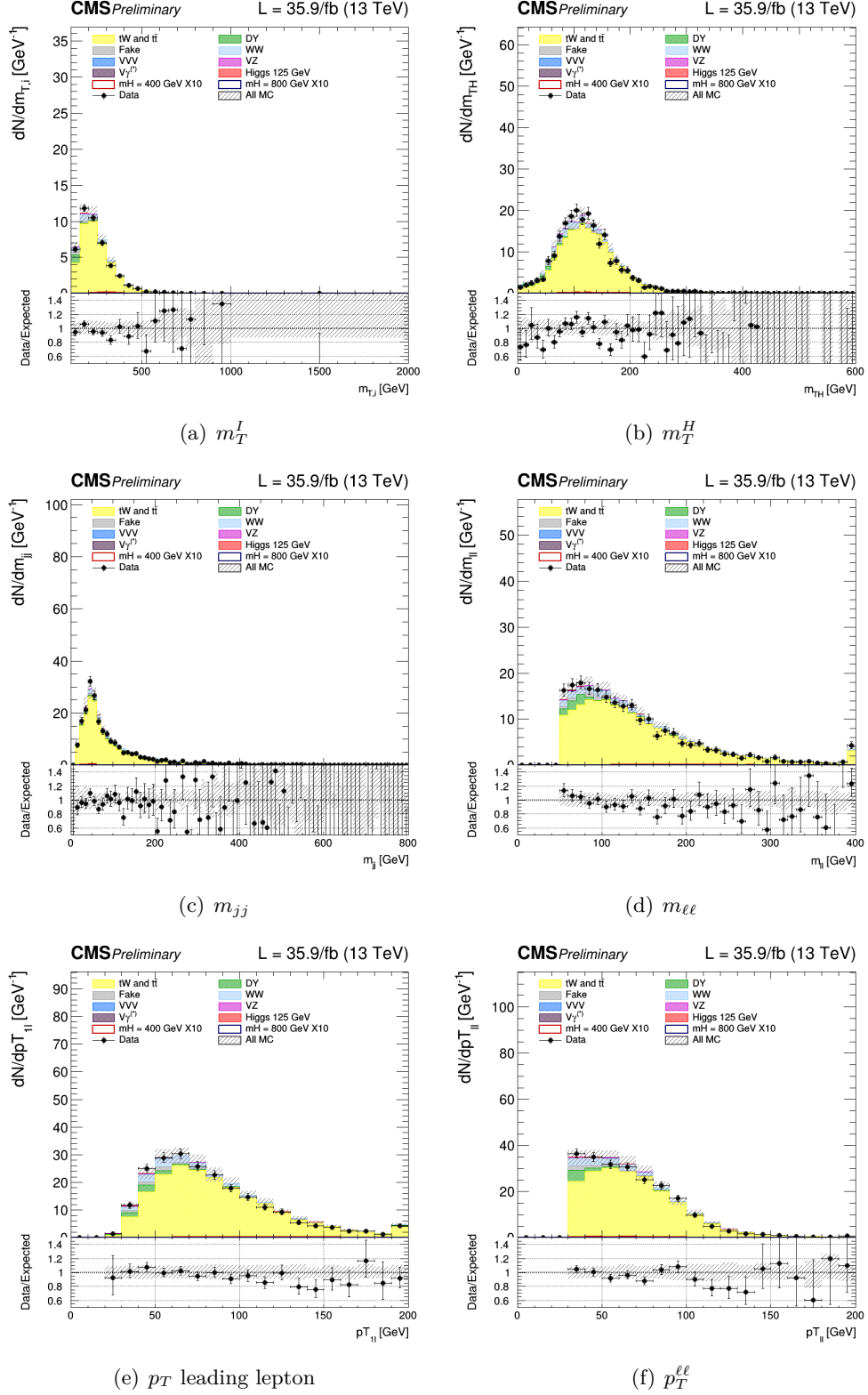


Figure 5.10. Control plots for several variables in the Top enriched phase space for events with 0 jet.

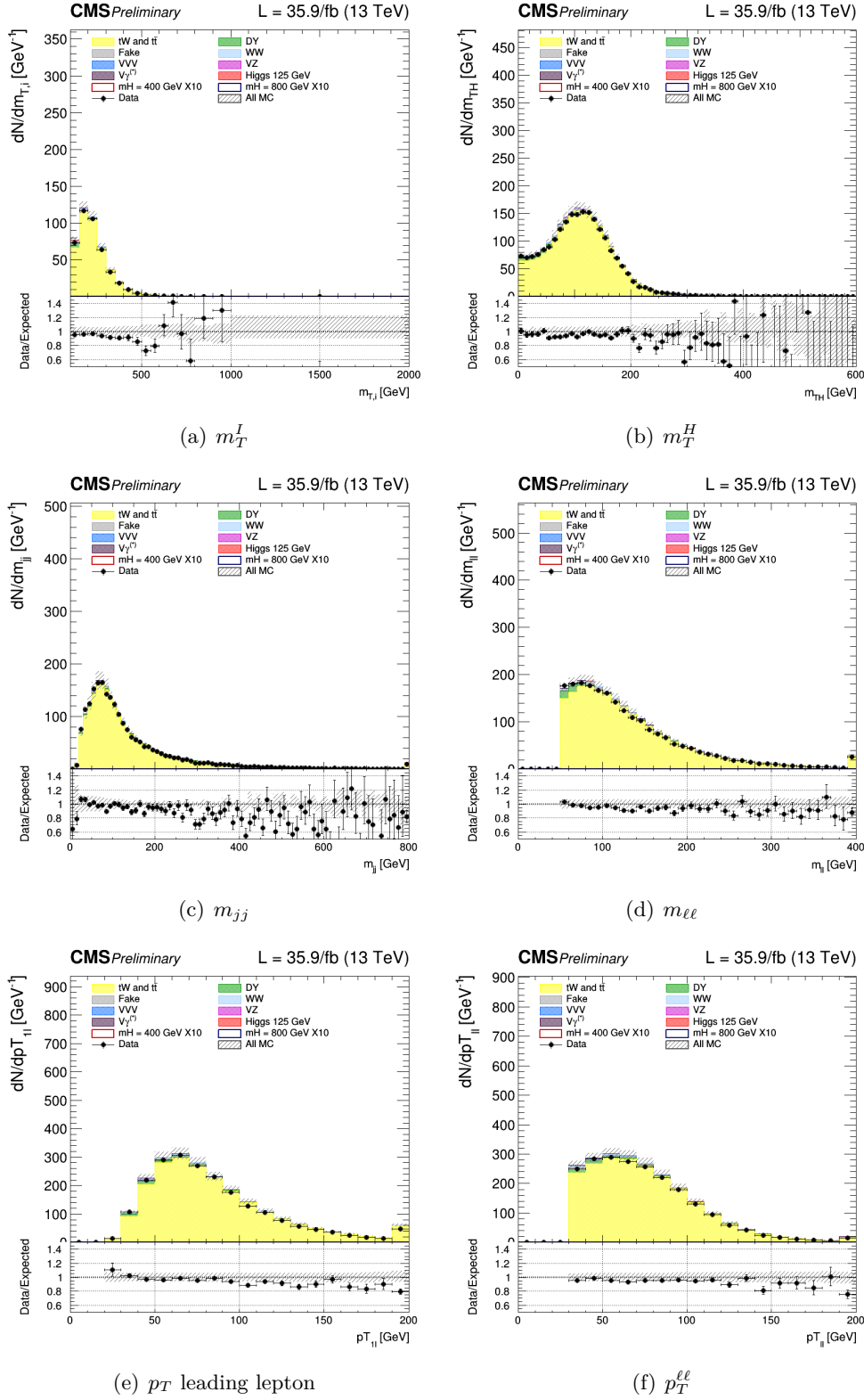


Figure 5.11. Control plots for several variables in the Top enriched phase space for events with 1 jet.

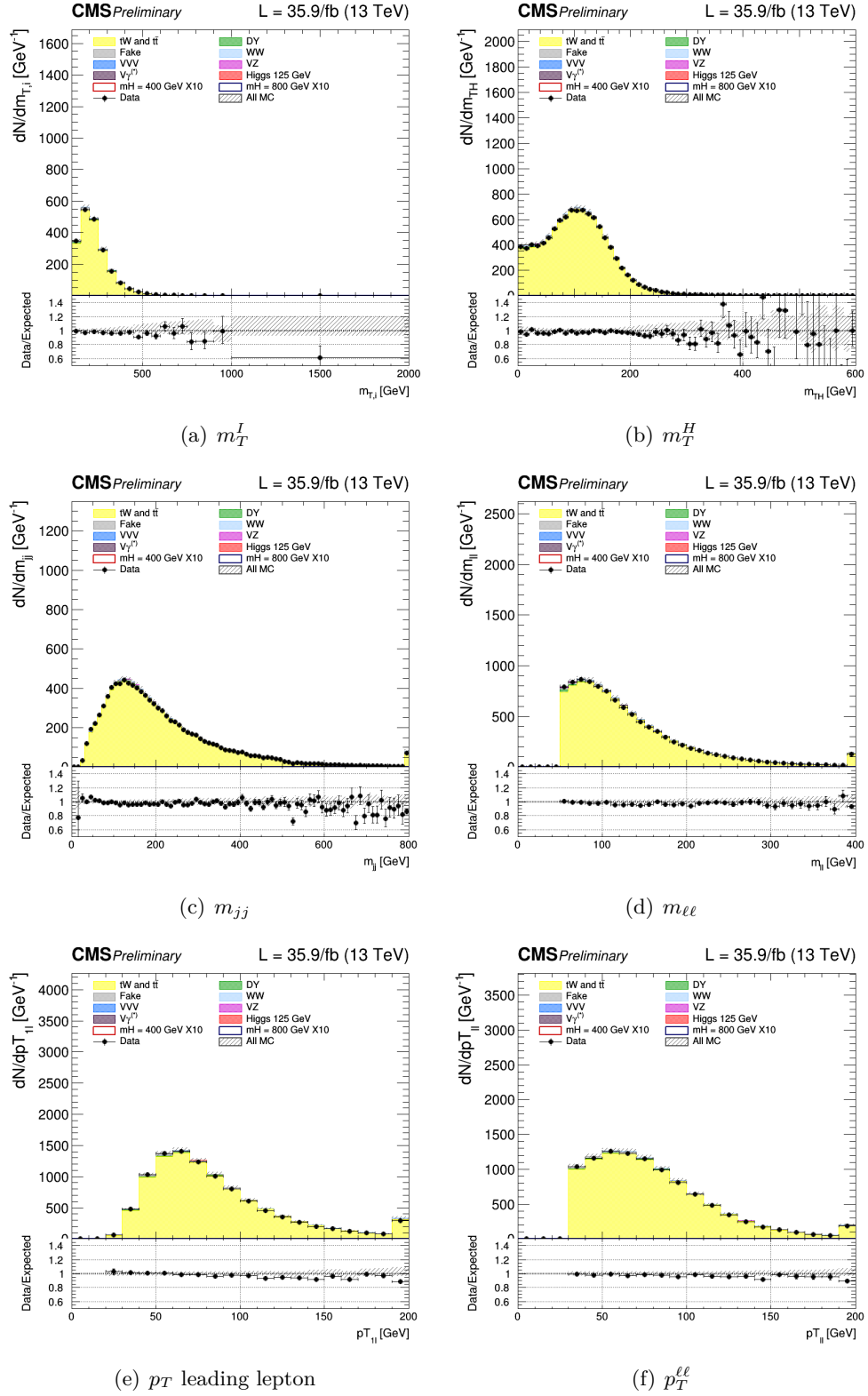


Figure 5.12. Control plots for several variables in the Top enriched phase space for events with 2 jet.

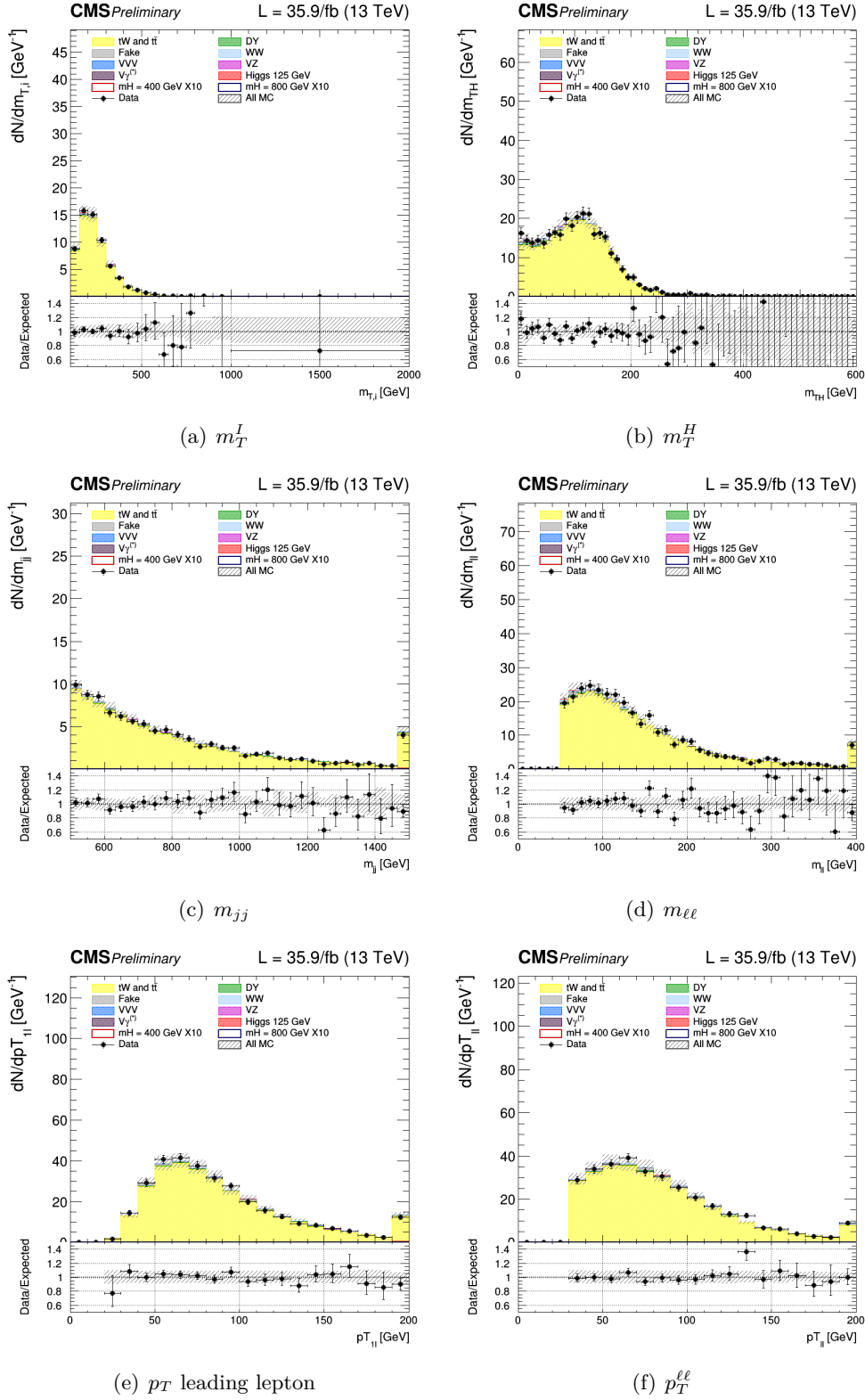


Figure 5.13. Control plots for several variables in the Top enriched phase space for events in VBF region.

5.5 Same Flavor final state

The analysis of the same-flavour final state $W^+W^- \rightarrow \mu^\pm\mu^\mp 2\nu$ and $W^+W^- \rightarrow e^\pm e^\mp 2\nu$ is described.

Signal region

Events are requested to pass single or double lepton triggers and all the physics objects definitions are the same as in the OF analysis. The final state consists of two well identified electrons or two muons with $p_T > 20$ GeV, opposite charge, and large missing transverse energy from the undetected neutrinos.

In addition to the backgrounds described for the OF final state, the background from $DY \rightarrow \mu^+\mu^-$ and $DY \rightarrow e^+e^-$ is very large in this final state. Indeed, due to this very large background, the SF analysis only targets the VBF topology, where the DY background is suppressed by the tight jet requirements. In addition, an invariant mass of the two leptons larger than 120 GeV is requested. The full selection, defined as the “WW SF selection”, is :

- Two isolated leptons with same flavor and opposite charge ($\mu^\pm\mu^\mp$ and $e^\pm e^\mp$);
- p_T of the leading and trailing lepton > 20 GeV;
- Third lepton veto: veto events if a third lepton with $p_T > 10$ GeV;
- $m_{\ell\ell} > 120$ GeV
- $p_T^{\ell\ell} > 30$ GeV;
- $MET > 50$ GeV;
- $m_T^I > 100$ GeV;
- At least 2 jets non b-tagged (according to cMVA2 loose WP) with $p_T > 30$ GeV.
- $\Delta\eta_{jj} > 3.5$;
- $m_{jj} > 500$ GeV;;

Similarly to the opposite-flavour analysis, the signal is extracted from a template fit of the m_T^I distribution. The m_T^I distributions have the following binning:

- **VBF**, [100,150,200,250,300,350,400,450,500,600,700,1000];

where the first number represents the lower edge of the first bin while the other numbers represent the upper edges. The last bin is an overflow bin. The binning has been chosen in order to have at least 10 expected Top-backgrounds event and at least 10 expected Drell-Yan events in each bin of the template.

The distributions for the signal region of m_T^I variable is shown in Fig. 5.5

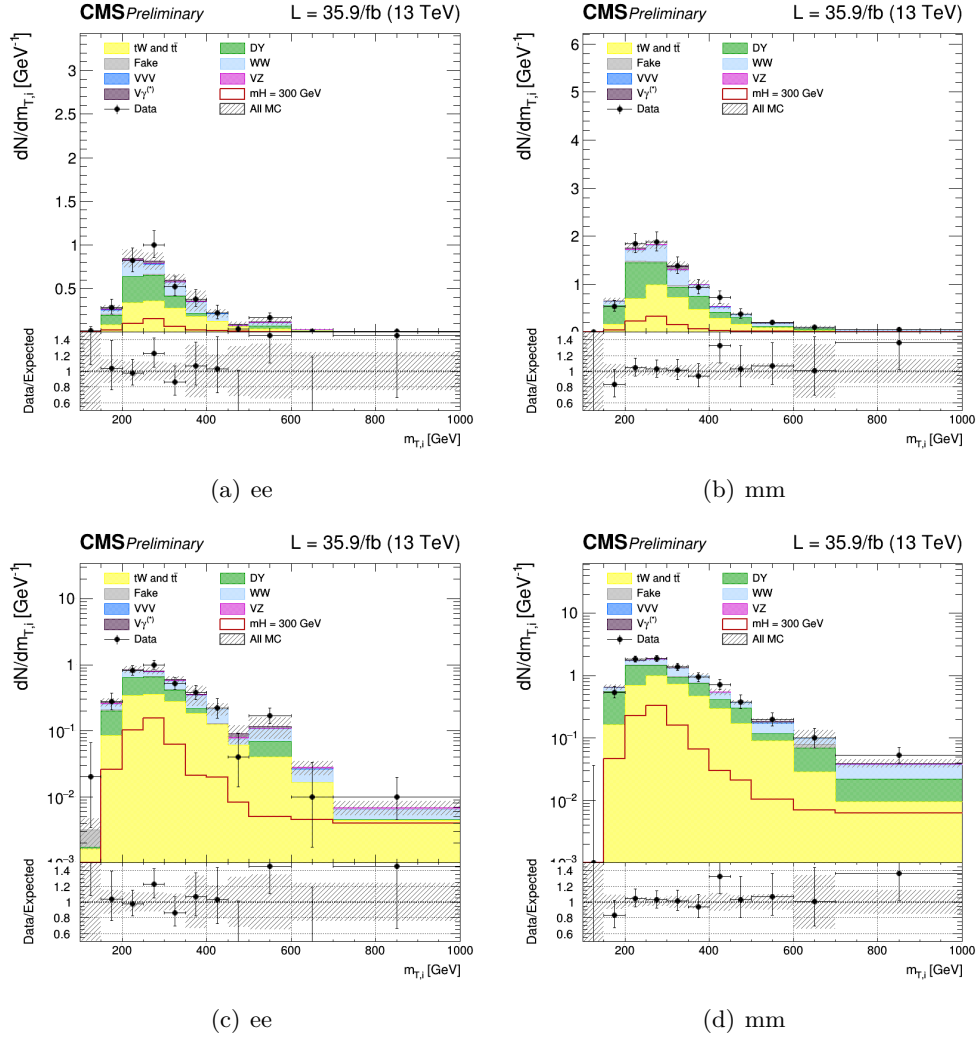


Figure 5.14. Unblinding distributions m_T^I in the signal region for ee and $\mu\mu$ categories in linear and log scale. The signal hypothesis corresponding to m_X of 300 GeV.

Drell-Yan control region

The main background for the SF analysis is the DY. A control region has been defined, as close as possible to the signal one to be used for the normalization of the DY background, separately for electrons and muons.

The control region is defined by the “WW SF selection”, except for the $m_{\ell\ell}$ requirement which is changed to $70 \text{ GeV} < m_{\ell\ell} < 120 \text{ GeV}$ to include the Z boson.

The missing transverse energy distribution in the data shows discrepancies respect to Monte Carlo simulation in ee and $\mu\mu$ Drell-Yan control regions. A correction is applied reweighting all the simulated samples with a weight per event which depends on the MET value. The weight is evaluated as the ratio between data, one subtracted all backgrounds except the DY, and the Drell-Yan itself, in each bins of the distribution, separately for ee and $\mu\mu$ categories. The weight is assumed to be linear as function of the MET value.

This kind of reweighting allows to correct for shape differences between data and MC, , Fig. 5.15.

The control plots for several variables in a Drell-Yan enriched phase space for the ee and $\mu\mu$ are shown in Figs. 5.17 for the dielectron case and Figs. 5.18 for the dimuon case. In general there is a good agreement between data and MC.

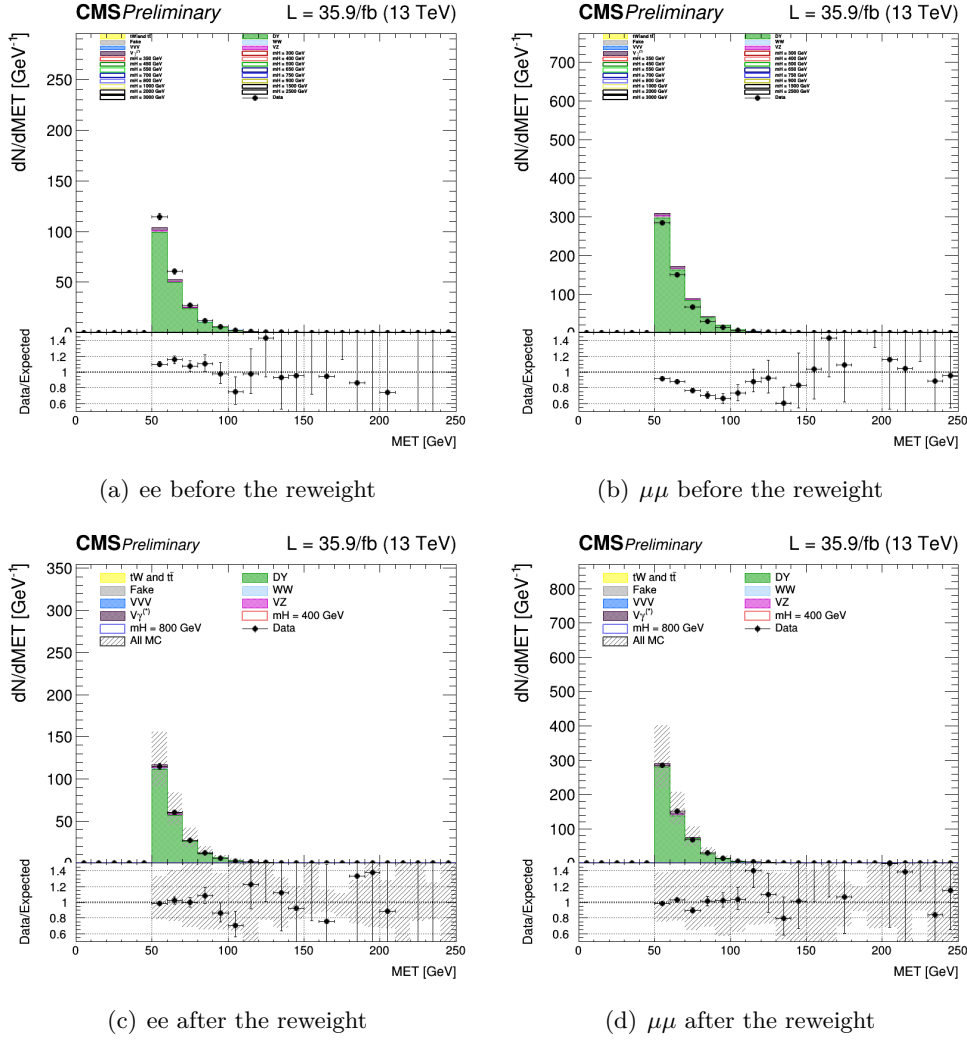


Figure 5.15. MET control plots for Drell-Yan for ee categories in *a* and for $\mu\mu$ in *b* before the reweight. In *c* and *d* the same distribution after the correction.

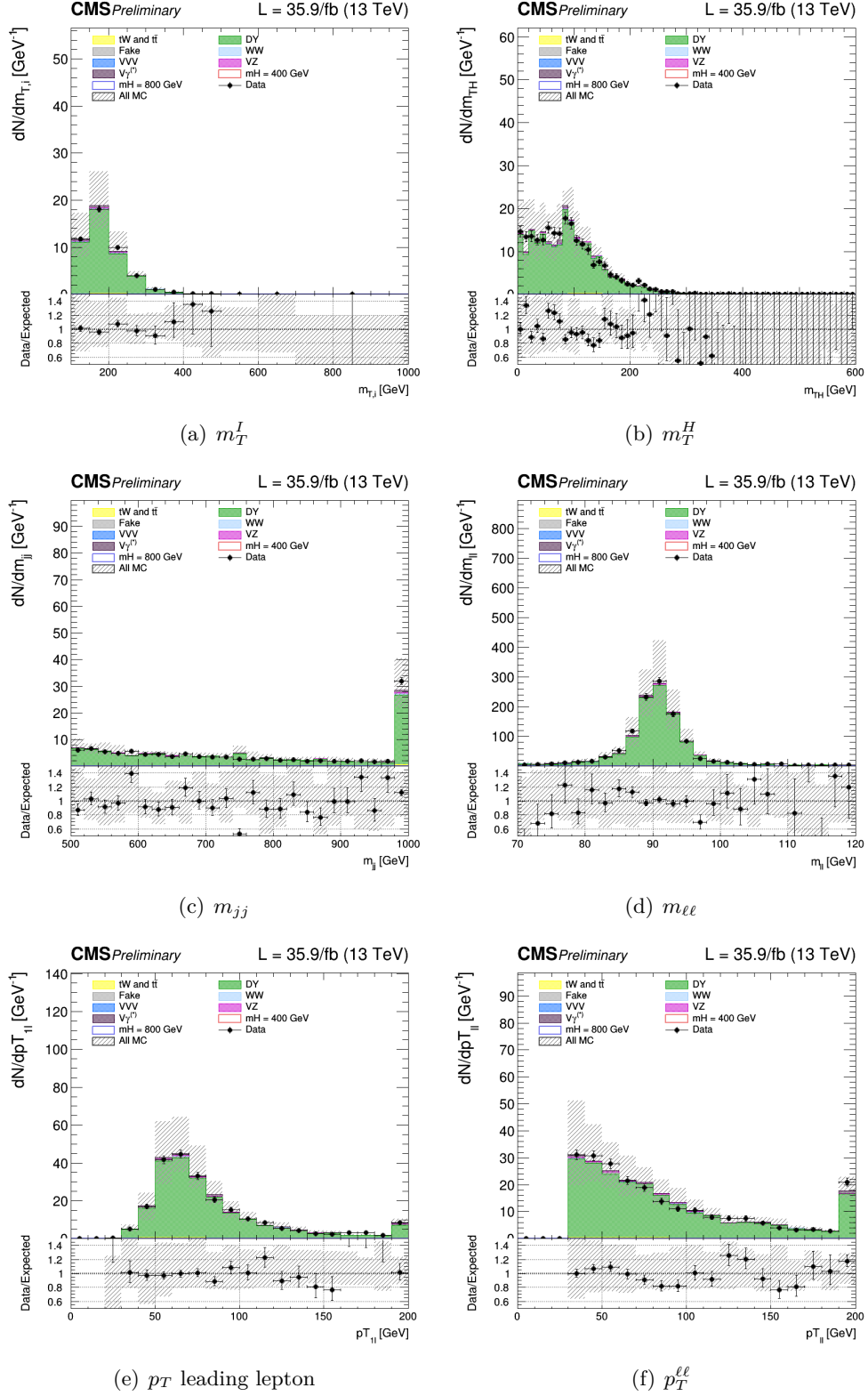


Figure 5.16. Control plots for several variables in a Drell-Yan enriched phase space for ee .

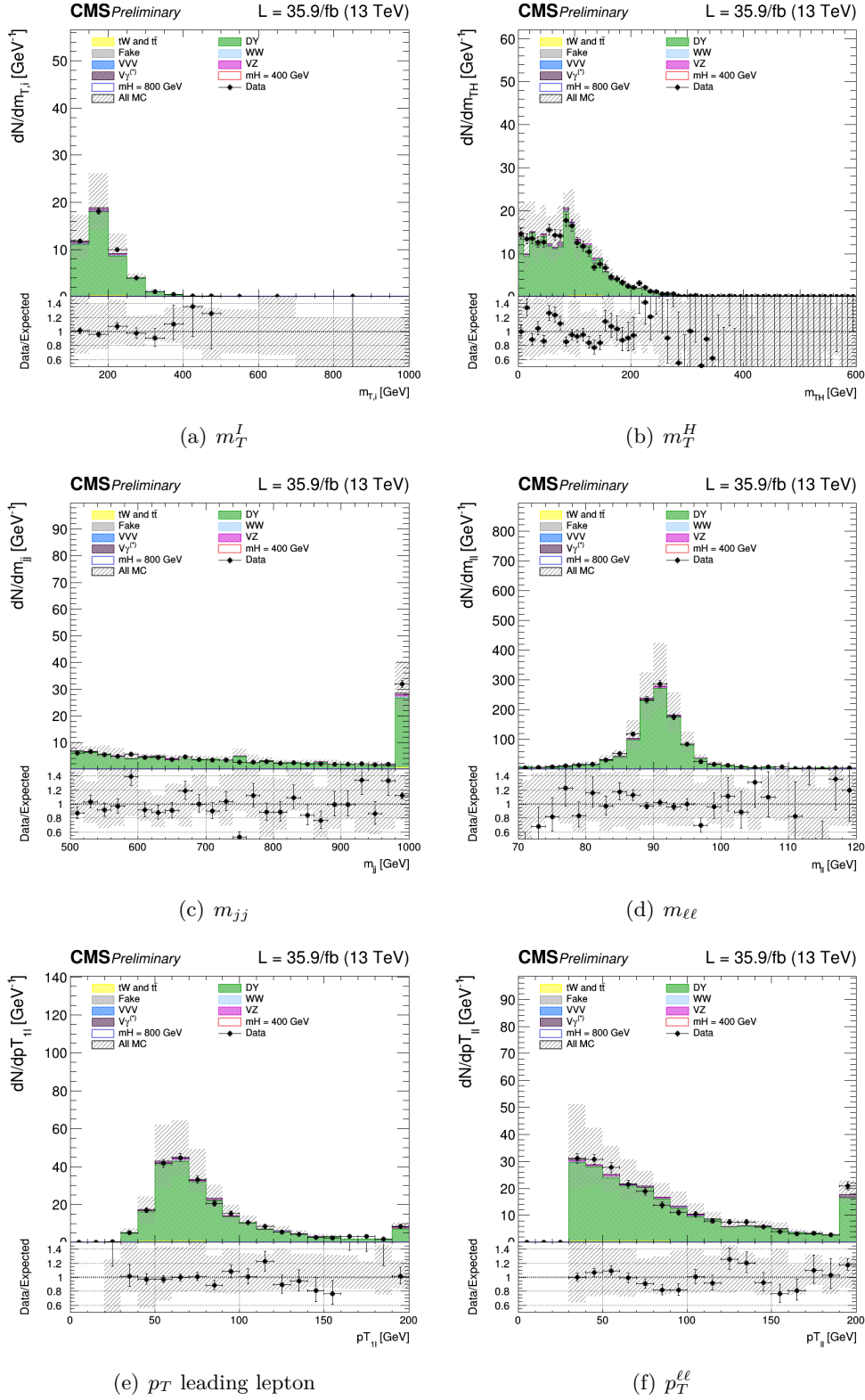


Figure 5.17. Control plots for several variables in a Drell-Yan enriched phase space for ee .

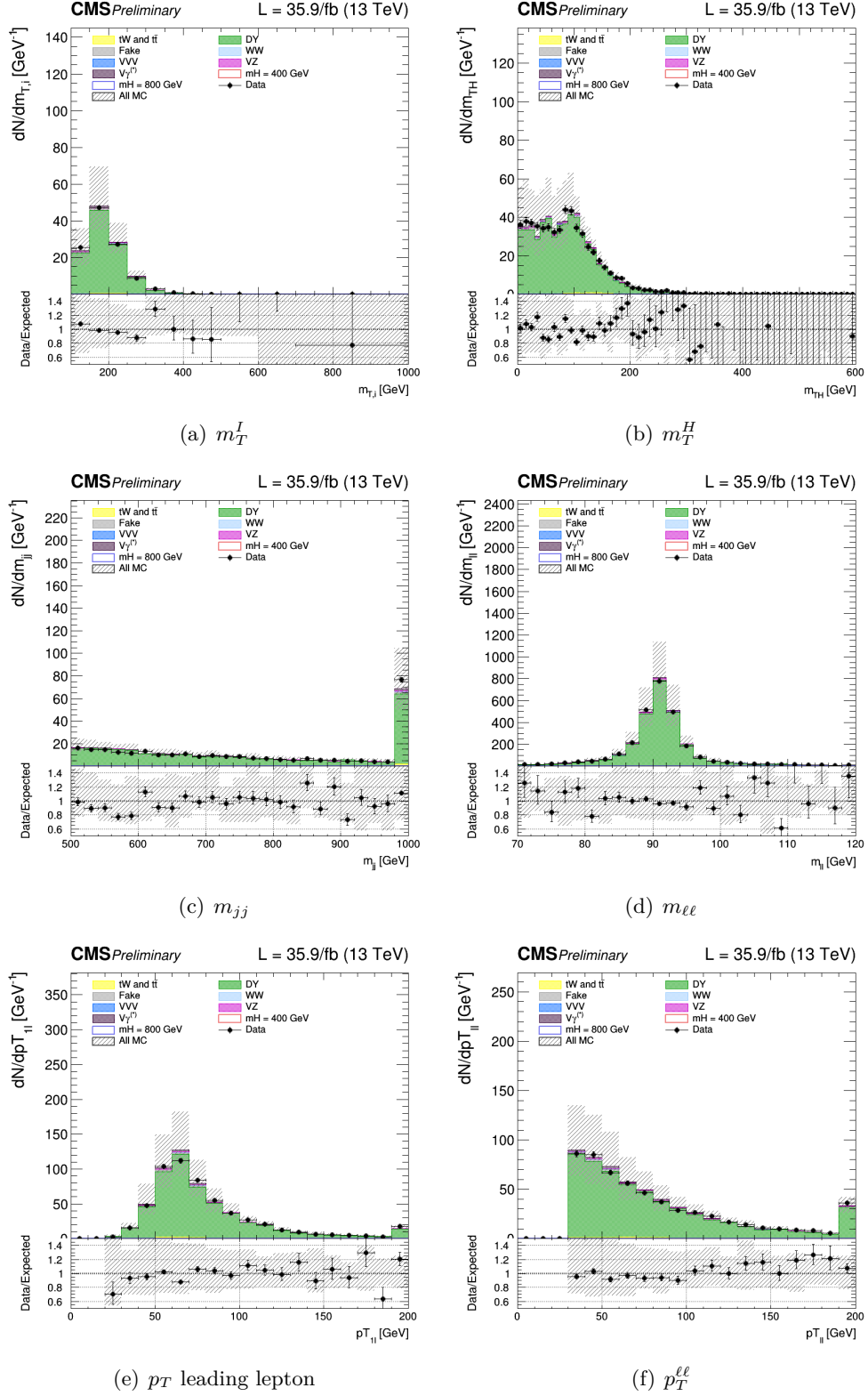


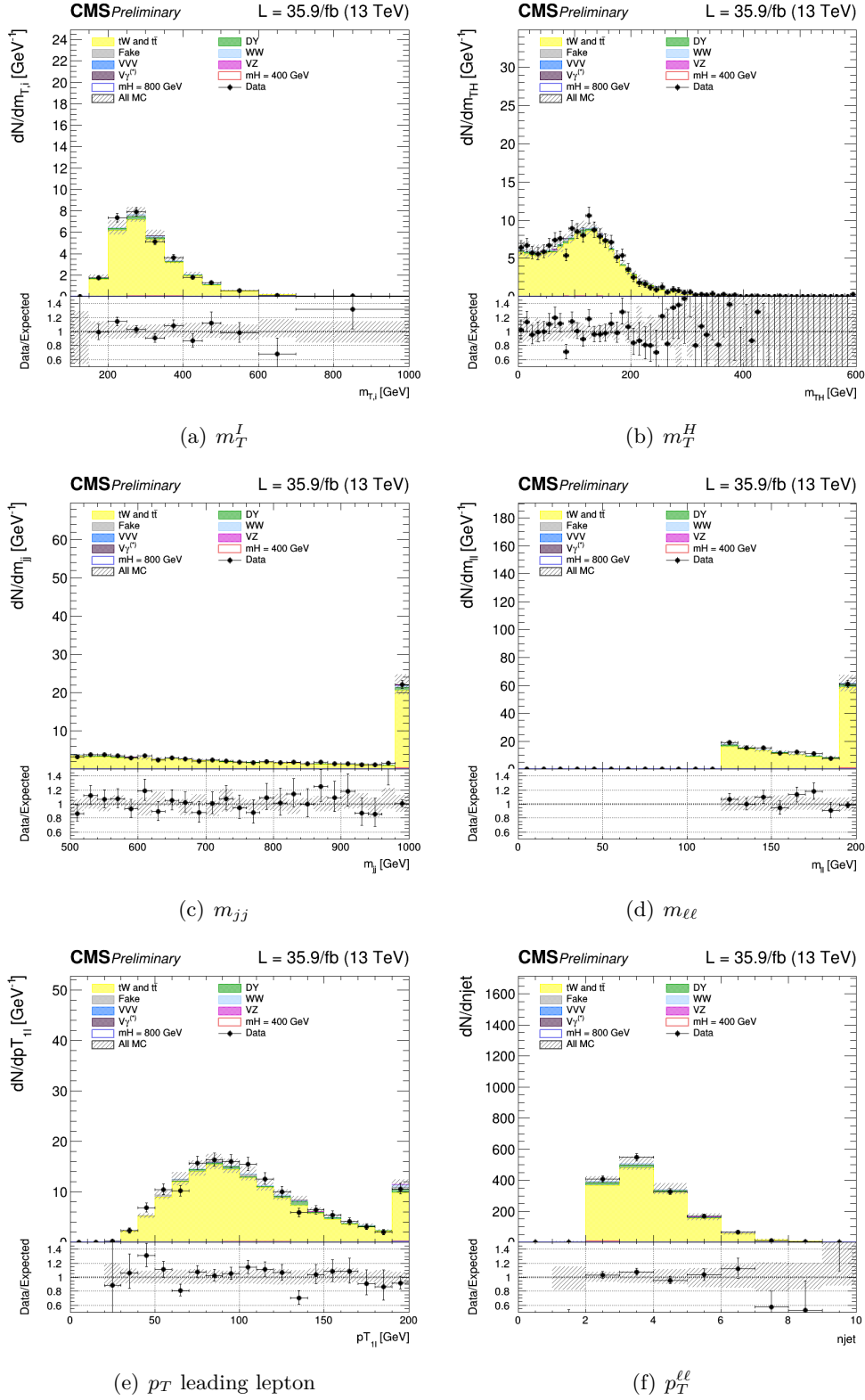
Figure 5.18. Control plots for several variables in a Drell-Yan enriched phase space for $\mu\mu$.

Top control region

A top-enriched control region is defined to normalize the top backgrounds, separately for electrons and muons. The “WW SF selection” is required with the inversion of the b-tagging requirement, i.e. the two jets are both requested to be b-tagged according to cMVA_{v2} loose WP.:

The control plots for several variables in a top enriched phase space for events are shown in the Figs. 5.19 for the dielectron case and 5.20 for the dimuon case. Good agreement is observed between data and MC.



Figure 5.20. Control plots for several variables in a Top enriched phase space for $\mu\mu$.

Chapter 6

Results and Interpretation

Appendix A

Special commands

Bibliography

- [1] Search for high mass Higgs to WW with fully leptonic decays using 2015 data. Technical Report CMS-PAS-HIG-16-023, CERN, Geneva, 2016.
- [2] HWW team. Common analysis object definitions and trigger efficiencies for the $H \rightarrow WW$ analysis with 2016 full data.
- [3] SM Higgs production cross sections at $\sqrt{s} = 13\text{-}14$ TeV. <https://twiki.cern.ch/twiki/bin/view/LHCPhysics/CERNYellowReportPageAt1314TeV>.